Hindawi
Geofluids
Volume 2023, Article ID 8927005, 16 pages
https://doi.org/10.1155/2023/8927005

Research Article

Engineering Characteristics and Application Analysis of Red Sandstone in the Lanzhou Metro

Yujie Li,[1] Zhongju Feng,[1] Yanpeng Zhu,[2] Pengyun Wei,[2,3] and Fudeng Zhao[2,4]

[1]*College of Highway, Chang'an University, Xi'an, Shaanxi 710064, China*
[2]*College of Civil Engineering, Lanzhou University of Technology, Lanzhou, Gansu 730050, China*
[3]*College of Water and Building Engineering, Tarim University, Alar, Xinjiang 843300, China*
[4]*Chongqing Major Construction Engineering Quality Inspection Co., Chongqing 400000, China*

Correspondence should be addressed to Yujie Li; lyjie2022@163.com and Yanpeng Zhu; zhuyp1@163.com

Received 30 June 2022; Revised 29 November 2022; Accepted 27 March 2023; Published 23 May 2023

Academic Editor: Dongjiang Pan

The water-rich red sandstone strata at the Lanzhou Metro site area have special engineering properties and vary greatly in their speed of disintegration when exposed to water. There is an urgent need for a comprehensive and systematic study of the engineering properties of red sandstone and their classification. From the disintegration speed of red sandstone encountered during the excavation of Lanzhou metro lines 1 and 2, the relationship between physical parameters such as particle size, composition, dry density, and permeability coefficient as well as mechanical parameters such as shear wave speed, dynamic penetration test (DPT), natural uniaxial compressive strength, and disintegration speed of red sandstone was analyzed through indoor and outdoor tests and geological exploration data statistics, and classification guidelines for red sandstone are given. The results show a significant correlation between dry density, permeability coefficient, natural uniaxial compressive strength, and disintegration speed. The red sandstone can be classified as I, II, and III according to the disintegration speed, dry density, permeability coefficient, and natural uniaxial compressive strength. The design of the foundations is differentiated according to the classification, and different support systems are used for the deep foundation pits of the metro stations. The category I red sandstone pit is supported by diaphragm walls with internal bracing, the category II pit by bite piles with internal bracing, and the category III pit by row piles with internal bracing. The study results can provide technical support and experience reference for the investigation, design, and construction of metro projects in similar red sandstone distribution areas.

1. Introduction

The hydrogeological environment of the site area along the Lanzhou metro is quite complex, and the special water-rich red sandstone strata of the northwest region were encountered during the construction process. The engineering properties vary widely: poor compaction cementation, high susceptibility to weathering after exposure, good mechanical properties before disturbance, rapid strength decline after disturbance, and disintegration into fluid-plastic loose sand in the presence of water [1–3]. This has led to many geological engineering problems. Furthermore, from the beginning of the construction of the Lanzhou-Chongqing railway tunnel to the Lanzhou metro, it is faced with these world-class engineering problems [4–11]: the excavation process of the red sandstone strata precipitation is yet to establish a mature theory and engineering method, resulting in in-pit collapse accidents in the construction of groundwater-rich areas prone to gushing water and sand; pit precipitation caused serious deformation of the surrounding ground surface, resulting in tilting of the surrounding houses and obvious cracks in the walls.

With the city's development and construction needs in mind, experts from both home and abroad have been researching the engineering problems of red sandstone encountered in the deep foundation pits of metro stations. For the engineering characteristics of red sandstone such as disintegration and permeability, Zhang et al. [12] verified that the Weibull distribution model can be applied to describe the evolution of rock particle disintegration and fragmentation using indoor static disintegration and perturbation disintegration tests. He et al. [13, 14] revealed the whole process of disintegration of red sandstones with different degrees of weathering in Red Hill Kiln by scanning electron microscopy (SEM) from microfabrication due to water absorption and swelling of hydrophilic minerals. Yu et al. [15] analyzed the variation pattern of red sandstone permeability during fracture evolution. Ma et al. [16] concluded that clay minerals influence the disintegration process of red sandstone by analyzing the rock properties such as basic physical indicators and microstructural parameters of red sandstone slopes. Zhao et al. [17] revealed the permeability characteristics of thermally damaged red sandstones under freeze-thaw cycles and different envelope pressures. Yin et al. [18] concluded that red sandstone disintegration is caused by particle bonding fractures when encountering water. The effect of water on the mechanical properties of red sandstone has also been the subject of numerous studies. Wang et al. [19] used uniaxial impact tests to analyze the strength, deformation, and damage mechanisms of three types of water-bearing red sandstone specimens under hydrodynamic coupling conditions. Wang et al. [20] obtained from tests that the peak strength and elastic modulus of red sandstone increase as the surrounding pressure increases, and the support structure increases the surrounding pressure to facilitate the stability of the red sandstone body. Jiang [21] suggested that water content and compaction are important factors affecting the strength and damage pattern of red sandstone. Tang et al. [22] investigated the effect of dry and wet treatments on the shear behavior of red sandstone fractures using direct shear tests and established an empirical relationship between the drying-wetting cycle and mechanical properties. Zhao et al. [23] studied the test method, mechanism, and characteristics of red sandstone disintegration in highway-simulated test embankments and then proposed an effective engineering classification method. The classification is not applicable to red sandstone in the Lanzhou area.

The current studies have been carried out on red sandstones in specific areas, whereas the red sandstone strata encountered during the excavation of Lanzhou metro lines 1 and 2 are inconsistently weathered in various regions, with significant variances in disintegration and permeability, necessitating classification and research. There is no complete construction experience to draw on for the design of deep pits in this particular stratum, and there is no systematic research into the engineering properties of red sandstone in the entire Lanzhou area. The engineering properties of the red sandstone are grasped through statistical analysis of sufficient exploration data, in-situ and indoor testing, and analysis of engineering examples, and the appropriate parameters are selected to classify it to provide technical support for proposing a set of reasonable groundwater control measures for red sandstone strata and the later investigation, design, and construction of metro projects in areas with a similar red sandstone distribution.

2. Distribution and Characteristics of Red Sandstone

2.1. Distribution of Red Sandstone. The red sandstone is a sedimentary rock formed in the Mesozoic, Cenozoic, Jurassic, Cretaceous, and other geological ages and is extensively found in the Shaanxi, Gansu, and Ningxia basins, the Sichuan basin, the western Yunnan region, and other areas in northwest China. The red sandstone in Gansu covers an area of about $8 \times 10\,km^2$, belonging to the Neogene to Jurassic, primarily the Middle and Upper Triassic strata. The tertiary (Neogene and Paleogene) red sandstone encountered in the Lanzhou metro project is a unique geotechnical layer that was uplifted during the neotectonic movement and subjected to long-term weathering, denudation, erosion, and cutting by the Yellow River to form a weathering layer, followed by the deposition of Yellow River terrace pebbles and a loose loess layer of the fourth series on its surface. The red sandstone is more than a kilometer thick and is widely distributed in a wide area of Lanzhou, from the east of the Xigu District to the west of Yantan in the Chengguan District. The degree of weathering of the various rock layers in each region is generally inconsistent, and the engineering properties vary significantly. There are 12 pits with red sandstone in a section of Line 1 from Culture Palace Station to Wulipu Station and a section of line 2 from Square Station to Yanbei Road Station. The water table, red sandstone, and bottom of the pit are buried at depths ranging from 4–11 m, 8-13 m, and 20-28 m, respectively.

The tertiary system of weathered red sandstone in the Lanzhou area has special engineering geological characteristics. When left undisturbed, the strength can meet engineering requirements, but it degrades rapidly when subjected to adverse changes in loading conditions, hydrogeology, and other conditions. It is prone to weathering when exposed and to engineering geological phenomena such as disintegration, softening, quicksand, and soil cavities when exposed to water. In particular, the dynamic changes in groundwater directly impact the construction schedule and safety of the metro. Additionally, the Yellow River crossing will have a significant impact on the physical and mechanical properties of the red sandstone, which will be harmful to the construction and operation of the metro. The ground investigation in the Lanzhou area revealed that the stratigraphy of the proposed project site within the exploration depth of 40 m mainly consists of Quaternary Holocene artificial fill, alluvial pebbles, and Tertiary Palaeocene to Eocene sandstones. Figure 1 shows the geological formations. The depth of groundwater dive level measured during the investigation is 3.6-5.0 m; the aquifer is mainly a pebble layer; the thickness of the diving aquifer is about 17 m; the sandstone under the pebble is a relative water barrier; and there may be local fracture water on top of the sandstone.

The specific hydrogeology of the Lanzhou area has led to many technical difficulties in the design and construction of the metro, such as the selection of support measures, methods of excavation of the foundation pit, groundwater treatment methods, and building protection. Improper handling poses a significant hidden danger to the station's safety and surrounding buildings. It is thus important to conduct relevant research on red sandstone.

2.2. Disintegration of Red Sandstone. The disintegration speed of red sandstone is closely related to the excavation and support of metro pits, so it is important to classify the

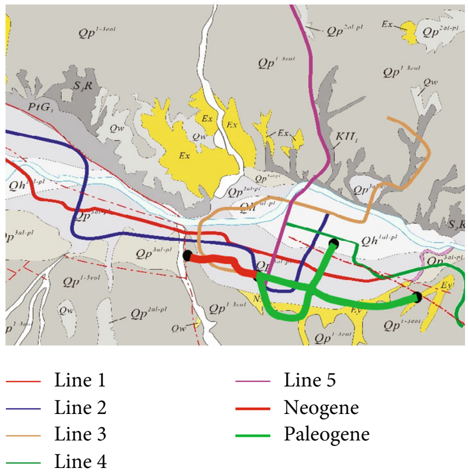

Figure 1: Geological map of the Lanzhou area. 1 : 50000. Qp$^{1\text{-}3eol}$ indicates the wind deposit layer; Qp$^{1al\text{-}pl}$, Qp$^{2al\text{-}pl}$, and Qp$^{3al\text{-}pl}$ indicate the alluvial-diluvial deposit layer; Qw indicates the Wuquan gravel layer; Nx indicates thick brownish-red bedded-block conglomerate interbedded with lenticular sandstone and mudstone; Ex indicates the purple-red block with a crisscross bedding coarse sandstone intercalated with medium thick fine sandstone and mudstone; and Ey indicates purplish-red mudstone, siltstone, sandstone, and gypsum.

red sandstone according to the time and intensity of disintegration. In-situ soil samples were obtained from typical stations along the metro line where the red sandstone was disintegrated by water, including 10-11 m at the provincial government station and 12-13 m at Xiguanshizi and Yanbei Road stations, respectively. The disintegration test apparatus is shown in Figure 2 and consists of an electronic scale with an accuracy of 0.05 g, a measuring cup, a leaky net with a 5 mm grid aperture, and a bracket assembly. Measuring cups were filled with tap water and placed on an electronic scale. Bracket put the leaky net in the measuring cup. Place the undisturbed rock sample of red sandstone on the leaky net. The bracket assembly and the leaky net were not in contact with the measuring cup.

Place the device on a level surface and set the electronic scale to read 0. Fill the measuring cup with 2/3 of the volume of water (submerge the leaky net by about 10 cm), observe the electronic scale reading (no more than 2/3 of the range), and then set the electronic scale reading to 0. The weighed specimen was placed on the funnel and timed, with data observed and recorded at 10, 20, 30, 40, 50, 60, 75, 90, 105, 120, 140, 160, 180, 210, and 240 s, and every 30 s thereafter until 600 s or the completion of disintegration. When the disintegration time exceeded 10 min, data was recorded every 1 min thereafter; when the disintegration time exceeded 20 min, data was recorded every 10 min thereafter; When the disintegration time exceeded 1 h, data was recorded every 1 h until the disintegration was complete. When the disintegration time exceeded 24 h, data was recorded every 2 h until the disintegration was complete. During the observation process, if there was no change in the reading for 2 consecutive hours or if the change did not exceed 1 g, the soil sample was considered to be finished disintegrating and the observation was stopped.

The following is the electronic scale reading:

$$m = \rho_s v - \rho_1 v, \tag{1}$$

where ρ_s is the density of the soil sample, ρ_1 is the density of the water, and v is the volume of the disintegrated body or the volume of water drained by the disintegrated body.

$$v = \frac{m}{(\rho_s - \rho_1)}. \tag{2}$$

Disintegration rock sample quality is

$$m_b = \frac{\rho_s m}{(\rho_s - \rho_1)}. \tag{3}$$

Rock sample disintegration speed is

$$u = \frac{m_b}{t} = \frac{\rho_s m}{[(\rho_s - \rho_1)t]}, \tag{4}$$

where t is the disintegration time interval.

The experimental results are shown in Figure 3 .As soon as the rock masses at the provincial government station were placed in the water, it rapidly produced abundant bubbles. After soaking for 1 minute, the outer perimeter of the rock sample generated a large number of fissures, and accompanied by a large number of air bubbles. After soaking for 4 minutes, the bottom of the rock mass collapsed rapidly and massively, forming a mushroom shape. After soaking for 6 minutes, the rock sample almost completely collapsed, leaving only a small amount of soil with large cracks on the top. After 1 hour, the amount of disintegration did not increase, and disintegration was complete. As soon as the rock sample at Xiguanshizi Station was put into water, a lot of bubbles came out of the rock. After 1 hour of immersion, disintegration and shedding occurred at the fissures of the rock edge. Within 4 hours of immersion, the angularity of the rock sample disappeared, the amount of disintegration increased. After 24 hours of immersion, the amount of rock disintegration hardly increased any more, and disintegration was completed in 24 hours. As soon as the specimen at Yanbei Road Station was first placed in the water, there were only bubbles emerging from the local fissure. After soaking for 10 minutes, the local cracks disintegrated slightly. After soaking for 4 hours, cracks appeared at the top of the rock block, and a small amount of disintegration occurred along the edge. After 24 hours of immersion, the amount of disintegration hardly increased any more.

The experimental results show that the disintegration characteristics of the red sandstone vary significantly between sites, with the fastest disintegration speed and the worst rock quality at the Provincial Government Station, followed by Xiguanshizi Station and Yanbei Road Station, which have the slowest response and least disintegration with the best rock quality.

(a) Test device (b) Before disintegration (c) After disintegration

Figure 2: Disintegration experiment.

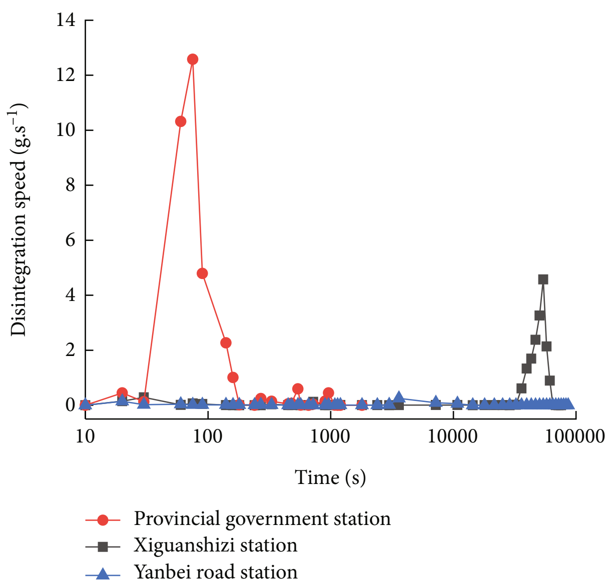

Figure 3: Test results of disintegration speed.

2.3. Preliminary Classification of Red Sandstone according to Disintegration Speed. In actual construction, the red sandstone of the Provincial Government Station pit disintegrates rapidly within a short period of time when it encounters water, causing serious engineering problems such as pit collapse and gushing water and sand. The red sandstone disintegration speed and intensity at Xiguanshizi Station are less than at the Provincial Government Station's, so there is a certain time to repair it. The red sandstone at Yanbei Road Station disintegrates slowly, is well supported, and has essentially no impact on construction. Because disintegration speed and pit support are closely related, it is important to classify the red sandstone according to the time and intensity of disintegration. The red sandstone encountered in the Lanzhou metro was initially classified into three categories based on the results of disintegration tests, as shown in Table 1.

According to the classification principle, the Provincial Government, Xiguanshizi, and Yanbei Road Stations are classified as Categories I, II, and III, respectively. But the principle only considers the effect of water on the disintegration speed of the red sandstone. Due to the change in sunshine, temperature, wind, and other factors in the actual geological exploration, the water content of red sandstone is different, resulting in a great difference in outdoor test results. The initial classification of red sandstone using disintegration speed is therefore only indicative. To make the classification scientific and reliable, it is necessary to further study the relationship between the physical and mechanical properties of red sandstone and the disintegration speed.

Table 1: Preliminary classification of red sandstone.

Category	Disintegration speed	Engineering issues
I	Rapid disintegration within 1 h	Serious
II	Partial disintegration within 1-24 h	Slight
III	Slow disintegration	Basically none

3. Correlation of Physical Properties of Red Sandstone with the Disintegration

3.1. Correlation of Particle Size of Red Sandstone with the Disintegration. Red sandstone samples were collected in the Provincial Government, Xiguanshizi, No. 5 Bus Company, and Yanbei Road Stations, at depths of about 15–18 m. According to the Standard for Geotechnical Test Methods (GB/T50123-1999), a sieve sizer with a pore size of 0.075/0.25/0.5/1/2/5/10 mm was used to analyze the particle size of red sandstone. Using the mass of specimens smaller than a certain particle size as a percentage of the total mass of the specimen as the vertical coordinate and the particle size as the horizontal coordinate, the particle size distribution curve is plotted on a single logarithmic coordinate, as shown in Figure 4.

The solid particles of the red sandstone form the red sandstone skeleton. The size of the grains and the percentage of different grains in the red sandstone play a decisive role in the physical and mechanical properties of the red sandstone. The disintegration of red sandstone satisfies the fractal property of broken block distribution

$$N = CR^{-D}. \quad (5)$$

R is the sandstone grain size in equation, N is the number of particles with a particle size greater than or equal to R, C is the proportionality constant, and D is the block fractal dimension.

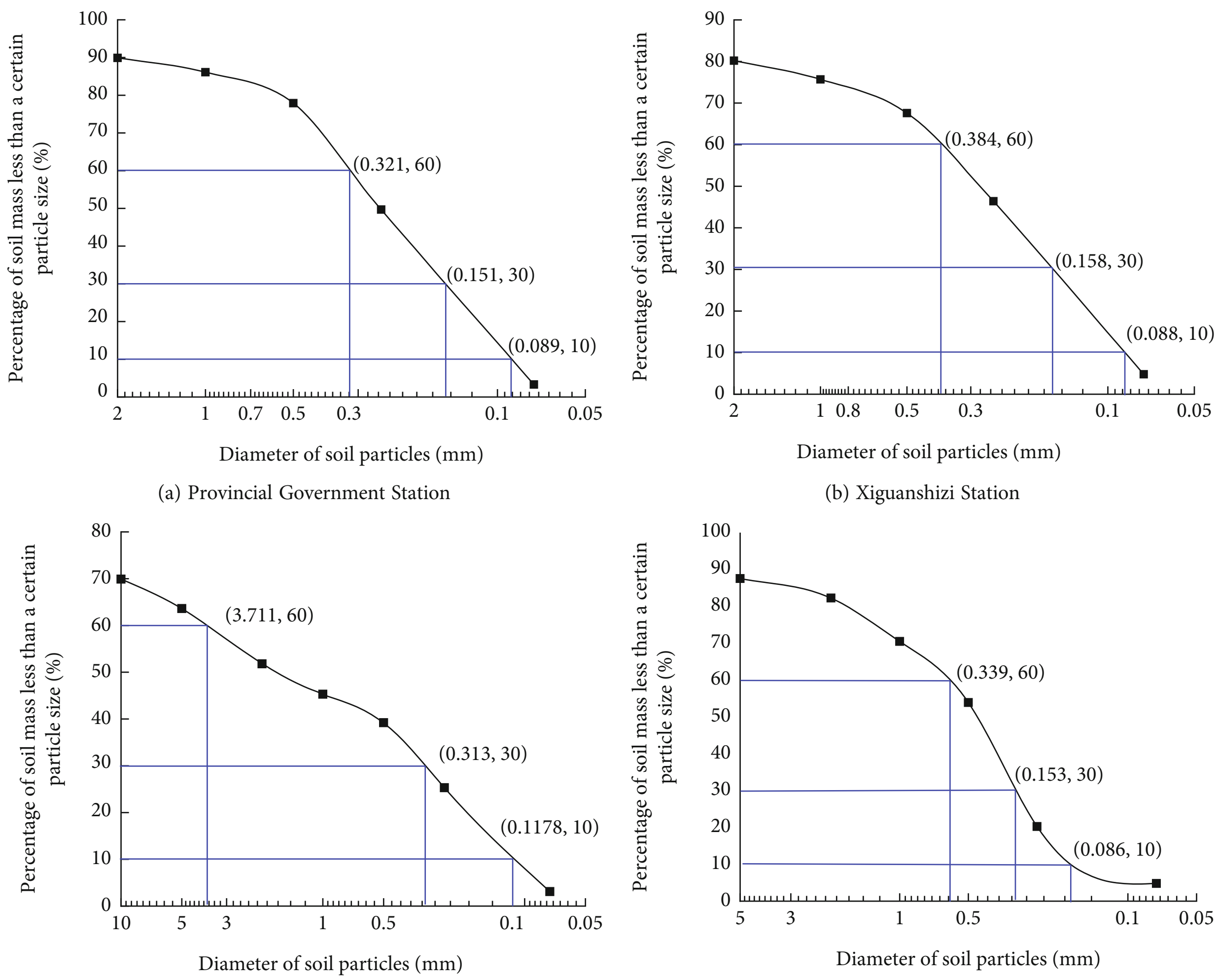

Figure 4: The red sandstone particle size distribution curve.

Assuming a total mass for the disintegrated specimen of red sandstone is M_T, the sieve aperture is R, and M_r is the cumulative mass of sandstone with a grain size less than R. M_T and M_r can be obtained by particle-size sieving tests.

$$\frac{M_r}{M_T} = 1 - \exp\left[-(R/R_{\max})^{\alpha}\right]. \tag{6}$$

α is the mass-frequency distribution index in equation. $R_{\max}$ is the average value of the largest particle size layer in particle size sieving. It can be assumed that $R/R_{\max} \ll 1$ for well-graded red sandstone. Expanding the power function of Equation (5) using the Taylor series, $(R/R_{\max})^{\alpha} \longrightarrow 0$. Then, Equation (6) can be expressed as

$$\frac{M_r}{M_T} = \left(\frac{r}{M_T}\right)^{\alpha}. \tag{7}$$

Taking the derivative of Equation (7) gives (8):

$$dM_r \propto R^{\alpha-1} dR. \tag{8}$$

Taking the derivative of Equation (5) gives

$$dN \propto R^{-D-1} dR. \tag{9}$$

The mass M increases with the number of particles N

$$dN \propto R^{-3} dM. \tag{10}$$

Substituting Equation (8) and Equation (9) into Equation (10):

$$R^{-D-1} \propto R^{-3} R^{\alpha-1} = R^{\alpha-4}, \tag{11}$$

$$D = 3 - \alpha. \tag{12}$$

Taking the derivative of Equation (7) gives (13):

$$\ln\left(\frac{M_r}{M_T}\right) = \alpha ln\left(\frac{R}{R_{\max}}\right). \tag{13}$$

M_r/M_T and $R/R_{\max}$ can be obtained from particle-size sieving tests. The value of α can be obtained by regression analysis of $\ln(M_r/M_T)$ and $\ln(R/R_{\max})$ scatter plots. The fractal dimension of each station is obtained, as shown in Table 2.

The fractal dimension is an important physical indicator of the fine physical properties of a rock. The higher the number of fractional dimensions, the more complex the internal structure of the red sandstone. Comparing the fractal dimension and disintegration speed of red sandstone at each station, it can be seen that the larger the fractal dimension, the smaller the disintegration speed. However, the fractal dimension of Bus Company No. 5 station is larger than that of Yanbei Road Station, and its collapse speed is smaller than that of Yanbei Road Station. Therefore, red sandstone cannot be classified according to fractal dimension.

3.2. Correlation of Mineral Composition of Red Sandstone with the Disintegration. Studies of rock composition have shown that the clay-grain mineral composition and microstructure of rocks are the main factors influencing the classification of the degree of weathering. The red sandstone composition of the typical engineering sites, Provincial Government, No. 5 Bus Company, XiguanShizi, and Yanbei Road Stations, was identified, and the main mineral composition was obtained, as shown in Table 3.

Quartz, potassium feldspar, plagioclase, and calcite are insoluble in water. Its influence on the disintegration of the red sandstone is not apparent from the mineralogical composition alone. Montmorillonite, kaolinite, and chlorite are all clay minerals with hydrophilic and adhesive properties. Previous studies have suggested that the immersion disintegration properties of red sandstone are mainly influenced by clay minerals such as kaolinite, montmorillonite, and illite [24]. The greater the content of hydrophilic montmorillonite, the more disintegrative the rock will be. The montmorillonite content of the red sandstone at the Provincial Government (category I), Xiguanshizi Station (category II), and Yanbei Road Station (category III) is 2%, 3%, and 10%, respectively. It can be seen that the higher the montmorillonite content, the slower the disintegration speed. The results of the analysis contradict previous studies. The kaolinite content of the red sandstones of categories I, II, and III is 3%, 8%, and 2%, respectively, which shows that there is no certain correlation between kaolinite content and disintegration speed. The chlorite content of the red sandstones of categories I, II, and III is 2%, 4%, and 1%, respectively, which shows that there is no certain correlation between chlorite content and disintegration speed. Therefore, red sandstone cannot be classified by mineral composition content alone.

3.3. Correlation of Dry Density of Red Sandstone with the Disintegration

3.3.1. Dry Density Analysis of Red Sandstone. Among the physical properties of rocks, density is related to the mineral composition and structure of the rock. Dry density reflects the degree of denseness of the arrangement of the rock grains. It gives a side view of the rock's microstructure and elucidates its physico-chemical properties. Dry density tests were conducted on samples collected from several types of red sandstone engineering sites. According to the Standard for Geotechnical Test Methods (GB/T50123-1999), the natural density ρ of the sample was measured using the ring-knife method, the moisture content ω was measured, and then the dry density was calculated using Equation (14). Four ring-knife specimens were chipped for each group for the natural density measured at each engineering site, while six porcelain dishes were used to determine the moisture content. The four natural densities and six water contents were recorded as a set of data, and six datasets were measured at each station. The test data outside the margin of error were excluded, and the results are collated in Table 4.

$$\rho_d = \frac{\rho}{(1 + 0.01\omega)}. \tag{14}$$

Table 1 compares the excavation of the red sandstone site at each station to the disintegration speed classification principle. It is concluded that the Provincial Government and Yanyuan Road Stations belong to category I, the XiguanShizi and Bus Company No. 5 stations belong to category II, and the Yan Bei Road Station belongs to category III. The experimental results show a correlation between disintegration speed and dry density values: the faster the disintegration speed, the lower the dry density value; the slower the disintegration speed, the higher the dry density value. Therefore, it is necessary to conduct a statistical analysis of the geological exploration data on dry density to investigate its relationship with disintegration speed and classification.

3.3.2. Analysis of Dry Density Exploration Data of Red Sandstone. The general characteristic index dry density data was collated according to the Standard for Geotechnical Test Methods (GB/T50123-1999), Equations (15)–(17) are often used to calculate their arithmetic mean $\bar{x}$, standard deviation s, and coefficient of variation c_v to discern their reliability.

$$\bar{x} = \frac{1}{n}\sum_{i=1}^{n} x_i, \tag{15}$$

$$s = \sqrt{\frac{1}{n}\sum_{i=1}^{n}\left(x_i - \bar{\bar{x}}\right)^2}, \tag{16}$$

$$c_v = \frac{s}{\bar{x}}. \tag{17}$$

Values measured outside the range of $\bar{x}\pm 3\,s$ were discarded, and the remaining data were evaluated for variability. When $c_v < 0.1$, the variability is small and the arithmetic mean is reliable; when $c_v \geq 0.1$, that is data clearly unreasonable is discarded.

Following the above, 1606 dry density data for 33 engineering sites of Lanzhou metro line 1 phase 1 and line 2 phase 1 were collected, as shown in Table 5. It can be concluded that the coefficient of variation in the dry density at each engineering site is less than 0.1. The arithmetic mean of all dry density data for each engineering site is used as a

Table 2: The fractal dimension of rock.

Rock sample	Provincial Government	Xiguanshizi	No. 5 Bus Company	Yanbei road
Fractal dimension (D)	2.29	2.52	2.76	2.61

Table 3: Quantitative analysis of whole rock minerals.

Engineering site	Montmorillonite (%)	Quartz (%)	Potash feldspar (%)	Plagioclase (%)	Calcite (%)	Kaolinite (%)	Chlorite (%)
Provincial Government	2	70	10	13	\	3	2
Xiguanshizi	3	60	10	12	3	8	4
Yanbei road	10	57	9	17	4	2	1

Table 4: Dry density test results.

Stations	Group number	Density/(g·cm^{-3})	Moisture content/(%)	Dry density/(g·cm^{-3})	Average/(g·cm^{-3})
Provincial Government	1	1.96	10.35	1.77	1.82
	2	2.00	8.66	1.84	
	3	2.00	7.09	1.87	
	4	2.01	10.47	1.83	
	5	2.06	12.27	1.8	
	6	1.99	10.05	1.81	
Yanyuan Road	1	2.06	3.98	1.82	1.84
	2	2.08	5.45	1.84	
	3	1.94	5.04	1.86	
XiguanShizi	1	2.28	12.32	2.03	2.01
	2	2.24	11.71	2.00	
	3	2.25	11.83	2.01	
	4	2.31	11.77	2.06	
	5	2.24	12.14	2.00	
	6	2.22	12.46	1.97	
No. 5 Bus Company	1	2.22	12.15	1.98	2.02
	2	2.12	11.77	1.90	
	3	2.22	11.36	1.99	
	4	2.23	13.41	1.97	
	5	2.33	9.85	2.12	
	6	2.35	10.10	2.13	
Yanbei Road	1	2.44	3.02	2.37	2.31
	2	2.33	5.19	2.21	
	3	2.43	2.74	2.36	
	4	2.42	4.37	2.32	
	5	2.38	3.82	2.30	

representative value for that engineering site, as shown in Figures 5 and 6.

From Figure 5, the dry density of the interval from Culture Palace to Xiguanshizi and the Xiguanshizi station are both greater than 1.9 g/cm^3. The maximum dry density at the remaining sites is 1.88 g/cm^3 at the Panxuan Road Station, indicating that they are all less than 1.9 g/cm^3. A comparison of the red sandstone site excavation at each site on line 1 against the disintegration speed classification guidelines reveals that all sites are classified as category I, except for the interval of Culture Palace to Xiguanshizi and Xiguanshizi Station, which are classified as category II. It can be

Table 5: Dry density data of lines 1 and 2.

Serial number	Engineering site	Number of samples	Average/$(g{\cdot}cm^{-3})$	Disintegration time
1	Interval of Cultural Palace to Xiguanshizi	40	1.83	<1 h rapid disintegration
2	Interval of Xiguanshizi to Provincial Government	94	1.73	
3	Provincial Government	45	1.71	
4	Interval of Provincial Government to Dongfanghong Square	225	1.76	
5	Dongfanghong Square	9	1.84	
6	Interval of Dongfanghong Square to Panxuan Road	44	1.71	
7	Panxuan Road	15	1.88	
8	Interval of Panxuan Road to Wulipu	13	1.81	
9	Wulipu	10	1.85	
10	Interval of Wulipu to Eastern Market	7	1.75	
11	Eastern Market	8	1.74	
12	Interval of Eastern Market to Gongxingdun	10	1.78	
13	Gongxingdun	6	1.71	
14	Interval of Gongxingdun to Jiaojiawan	18	1.82	
15	Jiaojiawan	9	1.8	
16	Interval of Jiaojiawan to Donggang	5	1.88	
17	Donggang	42	1.82	
18	Interval of Donggang to Youdiandalou	65	1.82	
19	Youdiandalou	39	1.8	
20	Interval of Youdiandalou to Train station	85	1.8	
21	Train station	49	1.73	
22	Interval of Train station to No. 5 Bus Company	21	1.78	
23	Interval of Dingxi Road to Wulipu	36	1.74	
24	Interval of Wulipu to Yannan	91	1.76	
25	Yannan Road	77	1.78	
26	Interval of Yannan Road to Yanyuan Road	35	1.83	
27	Yanyuan Road	96	1.81	
28	Interval of Yanyuan Road to Yanbei Road	57	1.81	
29	Xiguanshizi	45	2.02	1-24 h partial disintegration
30	No. 5 Bus Company	30	1.9	
31	Interval of No. 5 Bus Company to Dingxi Road	41	1.95	
32	Dingxi Road	115	1.9	
33	North side of interval of Yanyuan Road to Yanbei Road	17	2.19	Basically nondisintegrating
34	Yanbei Road	55	2.24	

observed that the dry density exploration values are all less than 1.9 g/cm^3 for category I and greater than 1.9 g/cm^3 for category II.

Figure 6 shows that the maximum dry density is 1.83 g/cm^3 between the interval of Donggang Station to Youdiandalou Station and the interval of Train Station to No. 5 Bus Company Station. The minimum value of No. 5 Bus Company Station to Dingxi Road Station is 1.9 g/cm^3. The maximum value is 1.84 g/cm^3 between the interval of Dingxi Road to Wulipu and the south side of the interval of Yangyuan Road to Yanbei Road. The minimum value is 2.17 g/cm^3 between the north side of the interval of Yanyuan Road to Yanbei Road and Yanbei Road. The site excavation of each engineering site in line 2 is compared to the disintegration speed classification guidelines, resulting in the interval of Donggang to Youdiandalou, Youdiandalou, the interval of Youdiandalou to Train Station, Train Station, the interval of Train Station to NO.5 Bus Company, the interval of Dingxi Road to Wulipu, the interval of Wulipu to Yannan, Yannan Road, the interval of Yannan Road to Yanyuan Road, Yanyuan Road, and the interval of Yanyuan to Yanbei belong to category I; NO.5 Bus Company, the interval of NO.5 Bus Company to Dingxi Road and Dingxi Road belong to category II; the north side of interval of Yanyuan Road to Yanbei Road and Yanbei Road belong to category III. That is, the red sandstone in category I has a

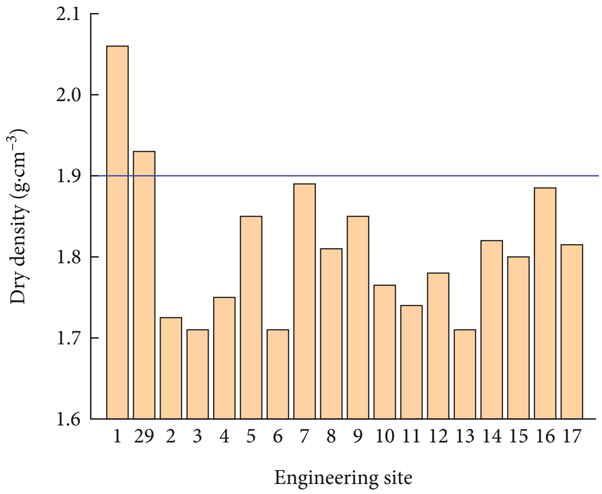

Figure 5: Statistics of dry density data for line 1.

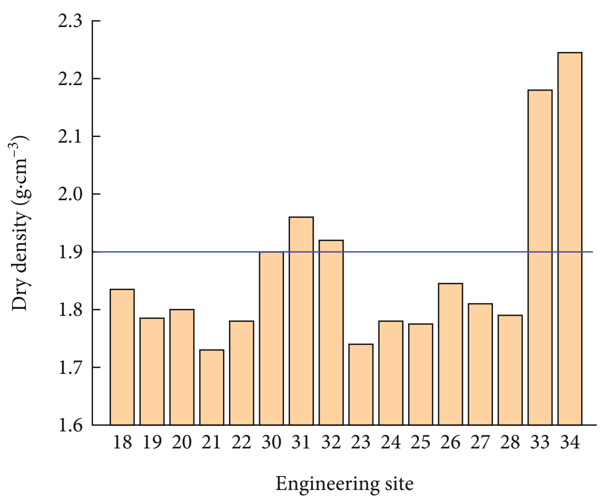

Figure 6: Statistics of dry density data for Line 2.

maximum dry density of 1.84 g/cm^3, all less than 1.9 g/cm^3, category II is all greater than 1.9 g/cm^3, and category III has a minimum value of 2.17 g/cm^3.

The dry density index is set at two boundaries: 1.9 and 2.1 g/cm^3, based on the regularity of the dry density geological exploration for lines 1 and 2. According to this limit, red sandstone can be divided into three categories: less than 1.9 g/cm^3 for category I, greater than 1.9 g/cm^3 but less than 2.1 g/cm^3 for category II, and greater than 2.1 g/cm^3 for category III.

3.4. Correlation of the Permeability Coefficient of Red Sandstone with the Disintegration. Indoor variable water head permeation tests were conducted at Yanbei Road, Xiguanshizhi, and the Provincial Government Stations, and Figure 7 shows the experimental setup. At each site, three ring-knife specimens were made, with three sets of readings for each ring-knife, each set including three data. The average of the three readings from each group is used as the permeability coefficient for the ring knife. Accordingly, nine average permeability coefficients can be obtained for each station. After excluding data outside the error, the data were collated to yield Table 6.

The site excavation of the red sandstone at each station is compared to the disintegration speed classification principle to obtain that the Provincial Government, Xiguanshizi, and Yanbei Road Stations belong to categories I, II, and III, respectively. The data in the table gives a permeability coefficient of 3.69×10^{-4}, 6.82×10^{-5}, and 2.57×10^{-8} cm/s at Provincial Government, Xiguanshizi, and Yanbei Road Stations, respectively. The faster the disintegration speed, the higher the permeability coefficient; the slower the disintegration speed, the lower the permeability coefficient, so it is necessary to use the permeability coefficient as one of the indicators for classification.

According to the above guidelines, setting two boundaries for the permeability coefficient index can classify red sandstone into three categories: less than or equal to 10^{-5} cm/s for category I, greater than 10^{-5} cm/s but less than 10^{-4} cm/s for category II, and greater than or equal to 10^{-4} cm/s for category III.

4. Correlation of Mechanical Properties of Red Sandstone with Disintegration

4.1. Correlation between Shear Wave Speed of Red Sandstone with Disintegration. 994 data points from 15 boreholes at 5 sites on line 1 and 2416 data points from 54 boreholes at 10 sites on line 2 were collected. The arithmetic mean of the shear wave velocities for different boreholes at the same depth was used as a representative value for that engineering site. Representative values for six selected depths (15-16 m, 20-21 m, 25-26 m, 30-31 m, 35-36 m, and 40-41 m) were obtained for statistical analysis. Figures 8 and 9 show the representative shear wave velocity values for the selected depths.

Based on the disintegration of the red sandstone excavated at each site and against the preliminary classification guidelines, it can be concluded that the red sandstone at Provincial Government Station and the interval of Dongfanghong Square to Provincial Government fall into category I, and the Xiguanshizi Station falls into category II. The shear wave velocity at Xiguanshizi Station is greater than that at Provincial Government Station, and the interval of Dongfanghong Square to the Provincial Government is in the range of 25-26 m, 30-31 m, and 35-36 m, whereas it is smaller in the range of 15-16 m and 20-21 m. The relative magnitude of the shear wave velocities at the three sites is not consistent at different depths. Different results are obtained at different depths if the red sandstone is classified according to shear wave velocity. Therefore, based on the statistical results of line 1, the shear wave velocity does not effectively distinguish between the different types of red sandstone.

Based on the disintegration of the red sandstone excavated at each engineering site and against the preliminary classification guidelines, it indicates that the red sandstone at Yanyuan Road Station falls into the category I, the No. 5 Bus Company and Dingxi Road Stations fall into category II, and Yanbei Road Station can be classified into category III. Figure 10 shows that the greater the depth of the same site, the greater the shear wave velocity. Comparing the

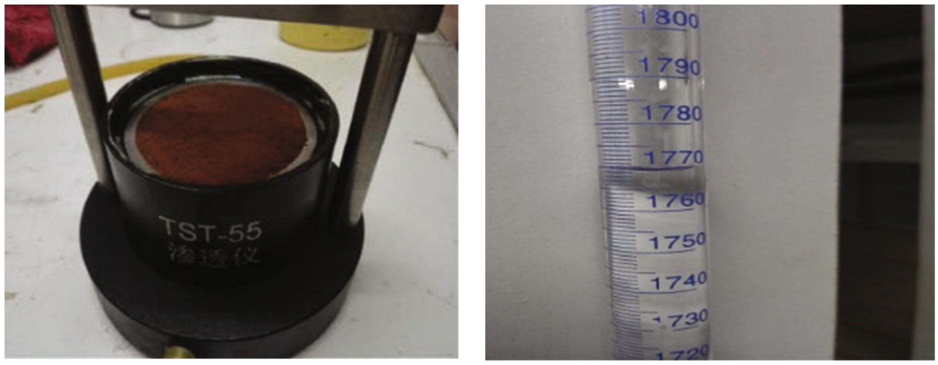

(a) TST-55 penetrometer (b) Pipe of variable water head

Figure 7: Permeability test of red sandstone.

Table 6: Test results of permeability coefficient.

Ring knife	a_1	a_2	a_3	b_1	b_2	b_3	c_1	c_2	c_3
Provincial Government	2.89×10^{-4}	2.77×10^{-4}	2.78×10^{-4}	5.22×10^{-4}	3.67×10^{-4}	5.88×10^{-4}	3.61×10^{-4}	3.19×10^{-4}	3.21×10^{-4}
Xiguanshizi	3.60×10^{-5}	4.17×10^{-5}	3.47×10^{-5}	7.34×10^{-5}	7.64×10^{-5}	7.72×10^{-5}	9.65×10^{-5}	9.00×10^{-5}	8.81×10^{-5}
Yanbei Road	2.31×10^{-8}	3.22×10^{-8}	2.12×10^{-8}	2.45×10^{-8}	3.63×10^{-8}	1.98×10^{-8}	2.73×10^{-8}	1.78×10^{-8}	2.95×10^{-8}

In the table, a_1, a_2, a_3, b_1, b_2, b_3, c_1, c_2, and c_3 represent three groups of data measured using ring cutters a, b, and c, respectively.

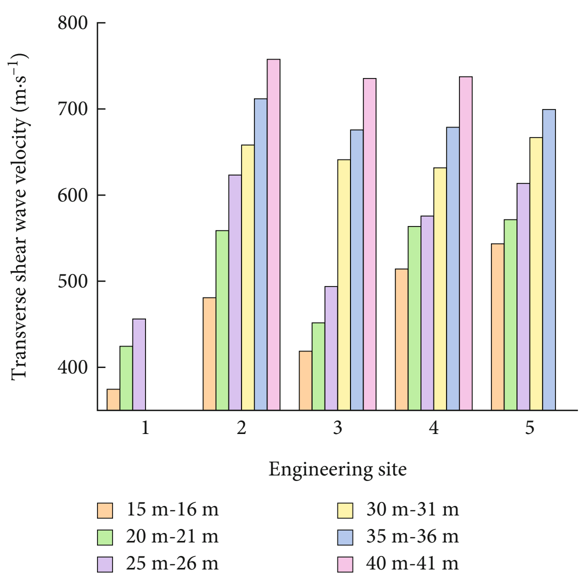

Figure 8: Statistics of shear wave velocity data from line 1. 1 means Cultural Palace to Xiguanshizi; 2 means Xiguanshizi; Xiguanshizi to Provincial Government; 4 means Provincial Government; and 5 means Provincial Government to Dongfanghong.

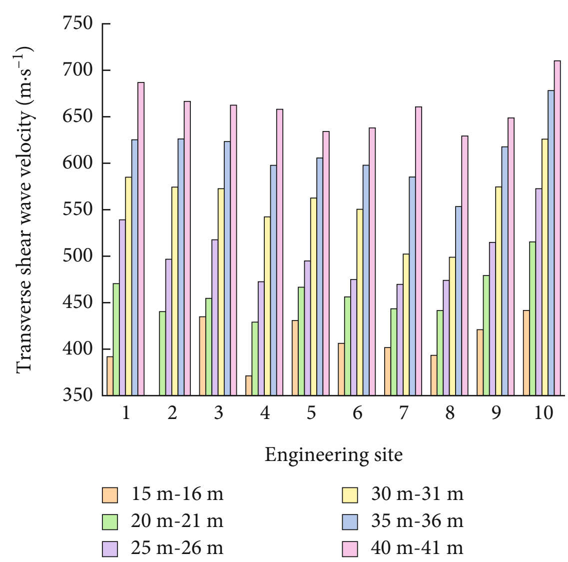

Figure 9: Statistics of shear wave velocity data from line 2. 1 means No. 5 Bus Company; 2 means No. 5 Bus Company to Dingxi; 3 means Dingxi Road; 4 means Dingxi to Wulipu; 5 means Wulipu to Yannan; 6 means Yannan Road; 7 means Yannan to Yanyuan; 8 means Yanyuan; 9 means Yanyuan to Yanbei; and 10 means Yanbei Road.

different sites, the shear wave velocities at different depth ranges are generally in line with the guidelines that Yanbei Road Station is the largest, followed by No. 5 Bus Company and Dingxi Road Stations, and Yangyuan Road Station is the smallest. Therefore, based on the exploration data from Line 2, the shear wave velocity can effectively distinguish between different types of red sandstone.

4.2. Correlation of Dynamic Penetration Test Value of Red Sandstone with the Disintegration. Based on the statistical analysis of the dynamic penetration test (DPT) results of the red sandstone layer on Lanzhou metro lines 1 and 2, the results of the same depth section (5 m is a depth section)

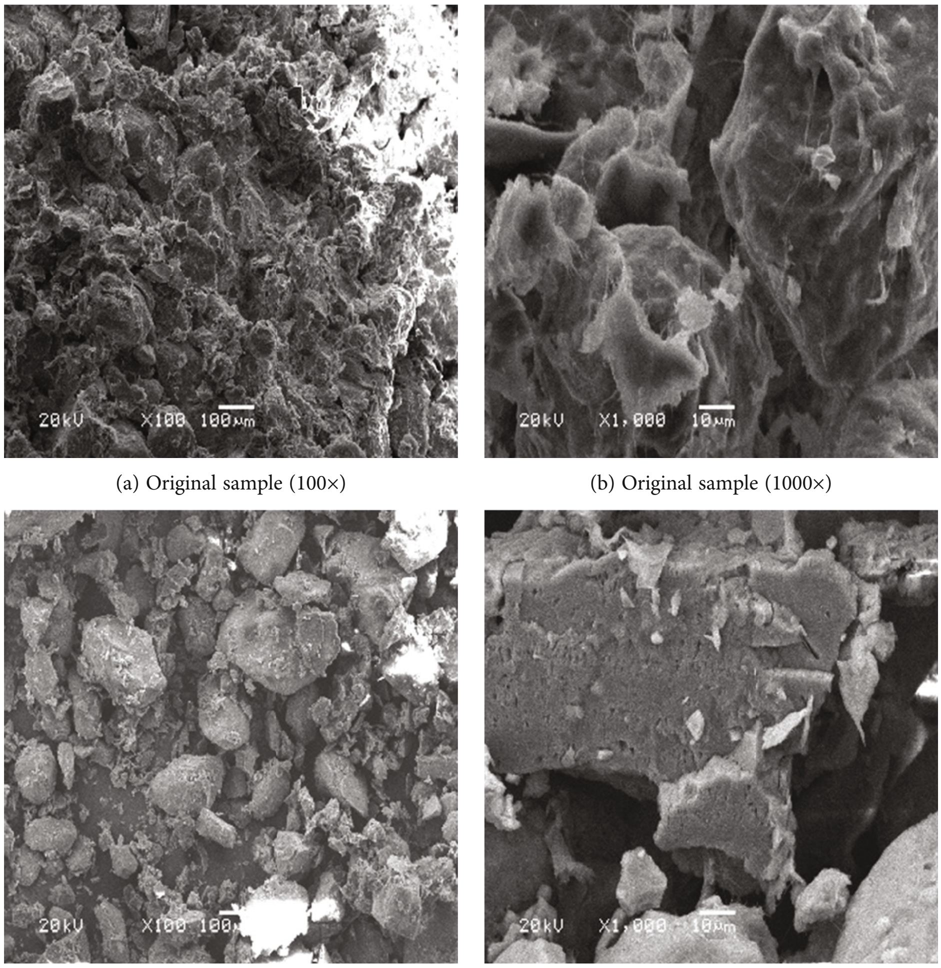

(a) Original sample (100×)

(b) Original sample (1000×)

(c) Disintegration sample (100×)

(d) Disintegration sample (1000×)

FIGURE 10: SEM analysis of red sandstone at the Provincial Government Station.

of different boreholes were collected as the representative values of the engineering site, as shown in Figures 11 and 12.

Figure 11 shows that the total number of hits at the same site increases with depth. The number of hits in the depth ranges of 20-25 m, 25-30 m, and 30-35 m for different engineering sites is basically the same for the interval of Wulipu to Eastern Market, Eastern Market Station, and the interval of Eastern Market to Gongxingdun. Other sites show waveform variations in the number of hits at adjacent sites. The excavation at each site is compared to the preliminary classification principle, and all sites can be classified as category II, except for the red sandstone at Jiaojiawan Station, which is classified as category I. However, Figure 11 shows that the DPT results of the Jiaojiawan Station are not significantly different from those of other stations. Therefore, the results of DPT cannot be used as a valid parameter for the classification of red sandstone.

Figure 12 shows the number of hits at the three sites in the interval of Dongfanghong Square to Youdiandalou, the interval of No. 5 Bus Company to Dingxi Road, and Dingxi Road Station, which are concentrated in the range of 33 to 40. The number of hits in the interval of Youdiandalou to Train Station and the interval of Train Station to No. 5 Bus Company is concentrated between 45 and 55. The number of hits at No. 5 Bus Company is concentrated between 55 and 80. It can be observed that the number of dynamic penetration hits fluctuates relatively widely along line 2, with no obvious guidelines. Additionally, the available data does not cover the existing line area.

Based on the disintegration of the red sandstone excavated on each site and against the preliminary classification principle, it can be concluded that the No. 5 Bus Company Station and the Dingxi Road Station belong to category II. In the depth range of 15-20 m and 20-25 m, the DPE result at NO. 5 Bus Station is overall relatively large, with a maximum value of 80 hits. In contrast, the DPE result at the Dingxi Road Station is overall smaller, with a minimum value of 35 hits. If the red sandstone is classified according to the DPT results, these two sites cannot be classified in the same category. Therefore, the classification of DPT results contradicts the principle of preliminary classification and cannot be used as one of the indicators for the classification of red sandstone.

4.3. Correlation of Natural Uniaxial Compressive Strength of Red Sandstone with the Disintegration. 536 natural uniaxial compressive strength data from 12 sites on Lanzhou metro

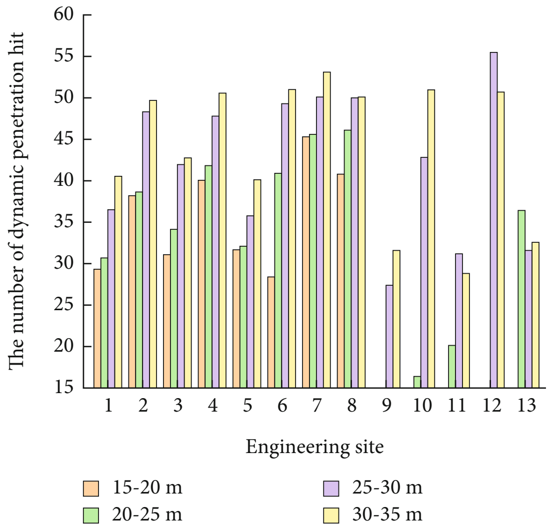

Figure 11: Statistics of dynamic penetration data for line 1. 1 means Dongfanghong Square; 2 means Dongfanghong to Panxuan; 3 means Panxuan Road; 4 means Panxuan Road to Wulipu; 5 means Wulipu; 6 means Wulipu to Eastern Market; 7 means Eastern Market; 8 means Eastern Market to Gongxingdun; 9 means Gongxingdun; 10 means Gongxingdun to Jiaojiawan; 11 means Jiaojiawan; 12 means Jiaojiawan to Donggang; and 13 means Donggang.

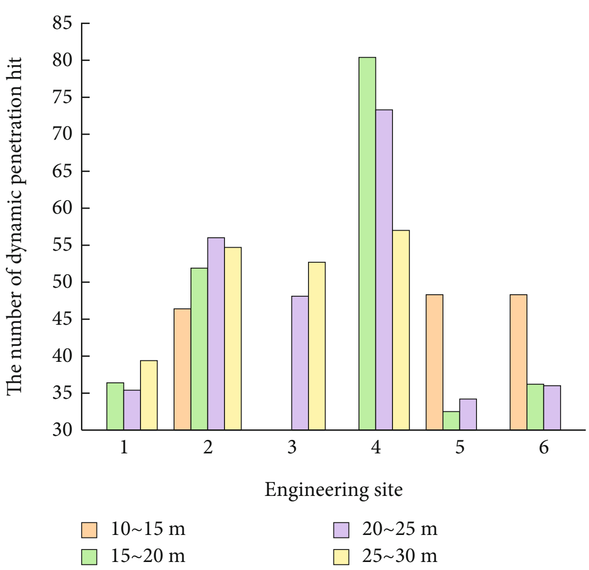

Figure 12: Statistics of dynamic penetration data from line 2. 1 means Donggang to Youdiandalou; 2 means Youdiandalou to Train station; 3 means Train Station to No.5 Bus Company; 4 means No.5 Bus Company; 5 means No.5 Bus Company to Dingxi; and 6 means Dingxi Road.

lines 1 and 2 were collected. The arithmetic mean of the test values within the same borehole depth range was chosen as a representative value of the natural uniaxial compressive strength for that site, as shown in Figure 13.

By comparing the excavation of the rock layers at each site with the preliminary classification principle, it was

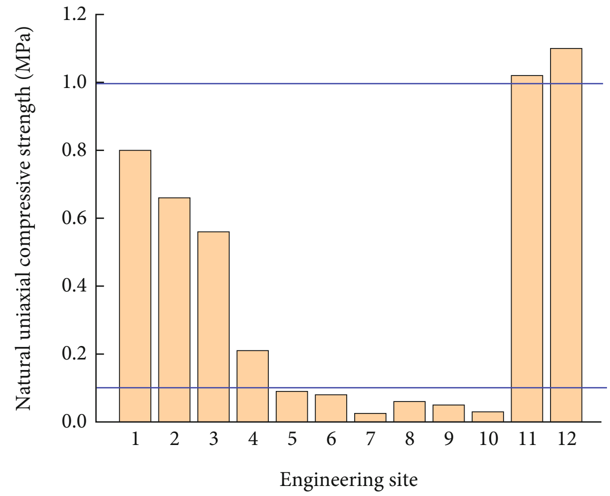

Figure 13: Statistics of natural uniaxial compressive strength data. 1 means Xiguanshizi; 2 means No.5 Bus Company; 3 means No.5 Bus Company to Dingxi; 4 means Dingxi Road; 5 means Dingxi to Wulipu; 6 means Wulipu to Yannan; 7 means Yannan Road; 8 means Yannan to Yanyuan; 9 means Yanyuan Road; 10 means Yanyuan to Yanbei; 11 means North of Yanyuan to Yanbei; and 12 means Yanbei Road.

obtained that the interval of Dingxi Road to Wulipu, the interval of Yannan Road to Wulipu, Yannan Road, the interval of Yannan Road to Yanyuan Road, Yanyuan Road, and the interval of Yanyuan Road to Yanbei Road belong to category I. Each natural uniaxial compressive strength is less than 0.1 MPa; Xiguanshizi Station, No. 5 Bus Company Station, and the interval of No. 5 Bus Company to Dingxi Road belong to category II. The compressive strength of each natural uniaxial is less than 1 MPa but greater than 0.1 MPa. The north side of the interval of Yanyuan Road to Yanbei Road and Yanbei Road station belong to category III. The compressive strength of each natural uniaxial is greater than or equal to 1 MPa.

In summary, setting two limits on the natural uniaxial compressive strength index allows the different properties of red sandstone to be distinguished: less than 0.1 MPa for category I, greater than 0.1 MPa simultaneously less than 1 MPa for category II, and greater than 1 MPa for category III.

5. Analysis on Disintegration Mechanism of Red Sandstone

SEM analysis was carried out on rock samples before and after disintegration at a magnification of 100 and 1000 times to analyze the disintegration process and mechanism of red sandstone. Figures 10–15 show the comparative analysis.

Figure 10 shows that the red sandstone at Provincial Government Station had a dense surface before the disintegration and that there are fissures and a large amount of filamentous cement, with a tight bond between the bulges and the dense layers. After the disintegration, the flocculent linkages between the particles disappear, and the surface shows fissures and voids, with disorderedly overlapping residual parts and a fall off of the bulges and dense layers.

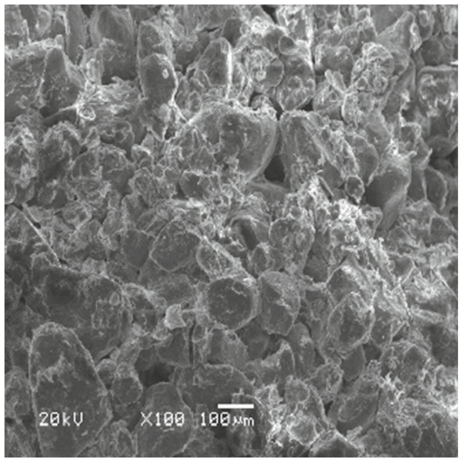

(a) Original sample (100×)

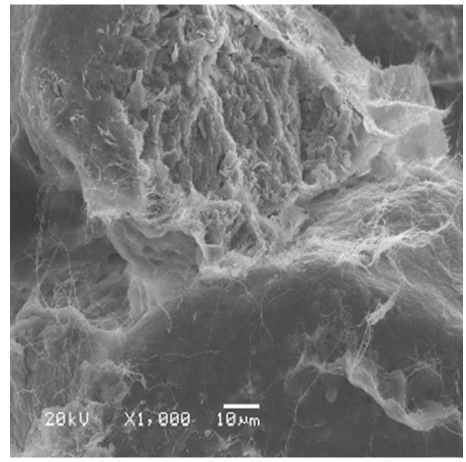

(b) Original sample (1000×)

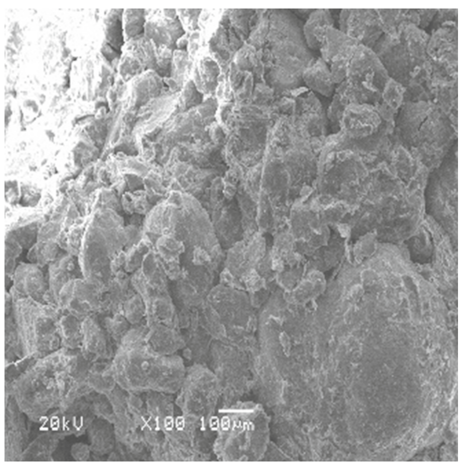

(c) Disintegration sample (100×)

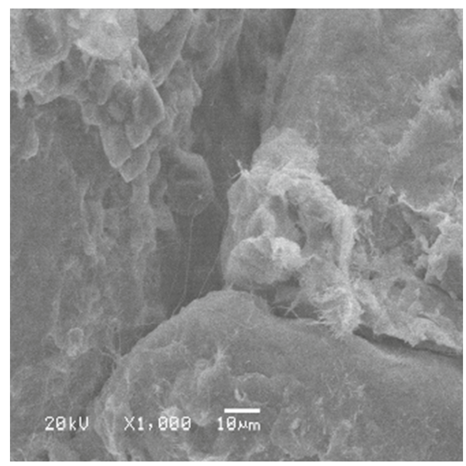

(d) Disintegration sample (1000×)

Figure 14: SEM analysis of red sandstone at Xiguanshizi Station.

Figure 14 shows that the red sandstone at Xiguanshizi Station has a smooth surface and a large amount of filamentous cement between the grains before disintegration, with a few bulges and a tight bond between the bulges and the dense layer, and few fissures. In contrast, the fissures become more numerous after the disintegration, the filamentous cement between the particles breaks off and significantly reduces, and the bulges fall off the dense layer.

Figure 15 shows that the red sandstone at Yanbei Road Station has a dense surface before disintegration, with a large number of flat, shallow honeycomb protrusions, and calcareous cementation has formed between the grains of each rock sample, with no filamentous cementation. The surface remains dense after disintegration, with a small amount of exfoliation in the protrusions but no cracks or porosity. There is essentially no difference in surface shape before and after disintegration.

In summary, there is a large amount of cement and more microcracks before the disintegration of red sandstone at Provincial Government Station, and the cement disappears and microcracks increase after the disintegration. There is a large amount of cement and fewer microcracks before the disintegration of the test specimen at Xiguanshizi Station, and the cement decreases and microcracks increase after the disintegration. The surface morphology of the test sample at Yanbei Road Station has little change before and after disintegration, little microcracks, and dense structure.

The flocculation binds the particle skeleton before disintegration, giving the red sandstone good integrity. The red sandstone itself has pores and fissures, and water penetrates into the rock through the shallow pores and fissures. The breakage of the nonhydrostable cementing bonds leads to a weakening of the interparticle forces and a reduction in interparticle adhesion. The flocculent linkages between the particles disappear, and the sandstone particles fall away from the rock surface to form a flatter water-rock interface after disintegration is complete. The causes of red sandstone disintegration at all three stations are essentially the same: an outward and inward interfacial process and a process of osmotic destruction by water absorption. This explains, from the perspective of microstructure, why the Provincial Government Station has the fastest disintegration of red sandstone, followed by Xiguanshizi Station and Yanbei Road Station.

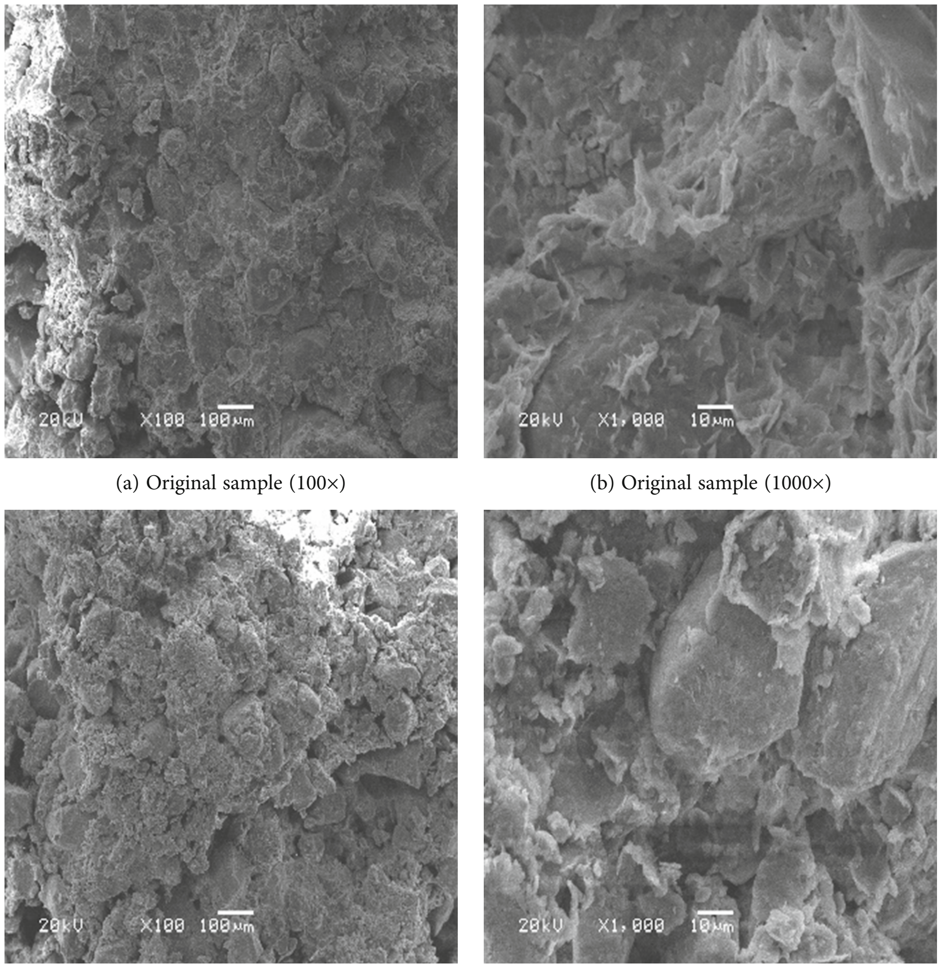

(a) Original sample (100×)

(b) Original sample (1000×)

(c) Disintegration sample (100×)

(d) Disintegration sample (1000×)

Figure 15: SEM analysis of red sandstone at Yanbei Road Station.

6. Engineering Application Effect and Evaluation

6.1. Engineering Classification of Red Sandstone. The Code of Practice for Geotechnical Investigations classifies rocks according to their hardness, integrity, weathering, and structural type. The saturated uniaxial compressive strength of the Lanzhou metro red sandstone is less than 5 MPa, making it an extremely soft rock. It is judged from the field characteristics to be a strongly weathered or fully weathered rock. This normative classification lacks relevance to the red sandstone of the area. To obtain a true and accurate picture of the differences between the different red sandstones, while maintaining a classification form that is simple and easy to use, a preliminary classification of red sandstone is based on the following principles: (1) simple and easy-to-test exploration data such as dry density, permeability coefficient, and natural uniaxial compressive strength are used as classification indicators; (2) comprehensive consideration of the relationship between the various factors influencing the stability of red sandstone engineering and selection of the main factors and the indicators of relative stability for a comprehensive evaluation; and (3) combining red sandstone classification with engineering applications.

In summary, to comprehensively reflect on the various factors affecting the stability of red sandstone projects, the red sandstone encountered in the construction of the Lanzhou metro was comprehensively classified into three categories using multiple indicators, as shown in Table 7. Different support systems were used for deep foundation pits in metro stations according to the red sandstone classification. Category I red sandstone disintegrates very rapidly when exposed to water and is highly permeable to water. The pit support system needs to be both supportive and water-blocking, and it is recommended to use a diaphragm wall with internal support. The category II red sandstone disintegration rate is second to none, the permeability is average, and the excavation has some time to salvage in case of water. It is recommended to use occlusal piles with internal support to save economy. The Category III red sandstone disintegrates slowly, has a very small permeability coefficient and is almost impermeable to water. It is recommended that the use of row piles with internal bracing support be sufficient to satisfy the supportability.

Table 7: Classification of red sandstone.

Category	Dry density/(g·cm^{-3})	Permeability coefficient/(cm·s^{-1})	Disintegration speed/h	Natural uniaxial compressive strength/MPa
I	≤1.9	≥10^{-4}	≤1	≤0.1
II	1.9-2.1	10^{-4}-10^{-5}	1-24	0.1-1
III	≥2.1	≤10^{-5}	Slow disintegration	≥1

Figure 16: Field seepage test using test pit method.

6.2. Application Effect of Youdiandalou Station. The water table of the Post and Telecommunications Building Station is 5.4-7.2 m deep, and the pit is about 25 m deep. From top to bottom, the layers are miscellaneous fill, a pebble layer, and a sandstone layer. According to the geological exploration data, the dry density of the strong weathered sandstone layer is 1.84 g/cm^3, and the permeability coefficient is 2.31×10^{-3} -5.79×10^{-3} cm/s. Preliminary judgment from Table 7 shows that it falls into the category I. The dry density of 1.79 g/cm^3 and permeability coefficient of 1.97×10^{-4} cm/s of the actual excavation tested, as well as the site conditions of the sandstone of the pit disintegrating in water, were consistent with the judgment. Accordingly, the enclosing measures adopted underground diaphragm walls; the cobble layer used tube well closed precipitation outside the pit; and the sandstone layer used in-pit vacuum light well point precipitation.

6.3. Application Effect of Dingxi Road Station. The stratigraphy of Dingxi Road Station consists of artificial fill, loess, pebbles, and sandstone. The dry density of the sandstone layer is 1.9 g/cm^3 according to the geological exploration data, and the red sandstone is tentatively judged to belong to category II. according to Table 7. The actual excavation was followed by a permeability test at a water table depth of 10-12 m, as shown in Figure 16. A permeability coefficient of 9.26×10^{-5} cm/s and a dry density of 1.99 g/cm^3 were measured, and the disintegration condition of the sandstone in contact with water was both consistent with category II. Accordingly, the station pit was supported by bored piles, steel pipe internal supports, and open drainage with collected water in the pit. The good engineering results show that the red sandstone classification method presented in this study is reasonable and effective.

7. Conclusions

The following are the conclusions from this study:

The water disintegration rate of the Lanzhou Metro red sandstone varies significantly and can be divided into three typical categories: disintegration completion times within 1 h; between 1 and 24 h; and greater than 24 h. The higher the dry density and permeability coefficient, the faster the disintegration speed; the lower the natural uniaxial compressive strength, the faster the disintegration rate. Red sandstone particle size distribution, mineral composition, shear wave velocity, and dynamic penetration test value have no effect on disintegration rate.

The disintegration process of the red sandstone was obtained by SEM analysis as both an outward-to-inward interfacial process and a process of osmotic destruction by water absorption. Water penetrates into the rock through shallow pores and fissures, and the fracture of the nonhydrostable cementing bonds leads to a weakening of the forces between the sandstone particles, the disappearance of the flocculent linkages between the particles, and the detachment of the sandstone particles from the rock surface.

By studying the relationship between various physical and mechanical parameters of red sandstone and disintegration, the red sandstone was classified into three categories according to dry density, permeability coefficient, disintegration speed, and natural uniaxial compressive strength. Category I red sandstone with a dry density of less than 1.9 g/cm^3, a permeability coefficient greater than 10^{-4} cm/s, a disintegration completion time of less than 1 h, and a natural uniaxial compressive strength of less than 0.1 MPa. Category II red sandstone with a dry density between 1.9 and 2.1 g/cm^3, a permeability coefficient between 10^{-4} and 10^{-5} cm·s^{-1}, a disintegration completion time between 1 and 24 h, and a natural uniaxial compressive strength between 0.1 and 1 MPa. Category III red sandstone with a dry density greater than 2.1 g/cm^3, a permeability coefficient less than 10^{-5} cm/s, a disintegration completion time greater than 24 h, and a natural uniaxial compressive strength greater than 1 MPa.

According to the classification of red sandstone, different support systems are used for the deep foundation pits of the metro stations, of which category I red sandstone pits are supported by underground diaphragm walls with internal support, category II by occluded piles with internal support, and category III by row piles with internal support. The classification method has been verified to be effective through engineering examples and can solve the difficult problems plaguing the construction of deep foundation pits in water-rich and soft rock formations in Lanzhou Metro, providing technical support and experience reference for metro projects in areas with similar red sandstone distribution.

Data Availability

The data used to support the findings of this study are available from the corresponding author upon request.

Conflicts of Interest

The authors declare that they have no conflicts of interest.

Acknowledgments

The study was supported by the Ministry of Education, Cheung Kong Scholar Innovation Team (No. IRT-17R51); Support Program of Gansu Province Science and Technology Program Funding (18YFIGA136); and Lanzhou Science and Technology Plan Project Funding (2018-4-12).

Supplementary Materials

1 plane layout of retaining structure of Youdiandalou Station. 2: support plane layout of Youdiandalou Station. 3: general plan of the main body and ancillary duct envelope of Dingxi Road Station. 4: design description of enclosure structure of Dingxi Road Station. *(Supplementary Materials)*

References

[1] Y. Zhou, H. J. Wang, and Y. P. Zhu, "Analysis of construction mechanical behavior of pile supporting structure for deep foundation pit of a subway," *Railway Engineering Journal*, vol. 36, no. 1, pp. 86–92, 2019.

[2] Y. P. Zhu, T. Ma, X. H. Yang, K. B. Yang, and H. M. Wang, "Shear strength test and regression analysis of red sandstone improved soil based on orthogonal design," *Journal of Geotechnical Engineering*, vol. 40, no. S1, pp. 87–92, 2018.

[3] Y. Zhou, N. Guo, Y. P. Zhu, and B. Yang, "Design and construction monitoring analysis of deep foundation pit support in Lanzhou metro test section," *Journal of Lanzhou University of Technology*, vol. 40, no. 4, pp. 110–114, 2014.

[4] Y. Zhou, N. Guo, and Y. P. Zhu, "Foundation pit support monitoring and numerical simulation of century avenue station of Lanzhou metro," *Journal of Railway Engineering*, vol. 1, pp. 82–88, 2014.

[5] F. D. Zhao, *Experimental Study and Analysis on Disintegration Characteristics of Red Sandstone in Deep Foundation Pit of Lanzhou Metro*, Lanzhou University of Technology, 2020.

[6] L. Lei, Y. L. Hua, G. P. Li, J. Qi, and D. Li, "Analysis and treatment of blind pipe blockage in Humaling tunnel of Lanzhou-Chongqing railway," *Modern Tunnel Technology*, vol. 57, no. 6, pp. 149–153, 2020.

[7] H. J. Bi, "Simulation study on groundwater seepage field of water sensitive sandstone in Humaling tunnel," *Railway Engineering Journal*, vol. 30, no. 12, pp. 64–68, 2013.

[8] W. Wang and Y. Zhou, "Application of computer simulation technology in the comparative analysis of excavation methods for large section railway tunnel," *Journal of Beijing Jiaotong University*, vol. 38, no. 4, pp. 148–153, 2014.

[9] L. L. Long, H. J. Liao, Y. P. Fu, and B. T. Deng, "Experimental study on effect of dry-wet state on brittle-ductile characteristics of red-bed soft rock," *Journal of Xi 'an Jiaotong University*, vol. 55, no. 4, pp. 162–171, 2021.

[10] X. H. Yao, J. Y. Xi, J. F. Guan, L. Liu, L. Shangguan, and Z. Xu, "A review of research on mechanical properties and durability of concrete mixed with wastewater from ready-mixed concrete Plant," *Materials*, vol. 15, no. 4, p. 1386, 2022.

[11] X. H. Yao, Z. W. Xu, J. F. Guan, L. Liu, L. Shangguan, and J. Xi, "Influence of wastewater content on mechanical properties, microstructure, and durability of concrete," *Buildings*, vol. 12, no. 9, p. 1343, 2022.

[12] Z. T. Zhang, W. H. Gao, Z. M. Zhang, X. Y. Tang, and J. Wu, "The evolution law of red sandstone particle disintegration and fracture based on Weibull distribution," *Geotechnical Mechanics*, vol. 41, no. 3, pp. 877–885, 2020.

[13] S. He, Z. D. Zhu, L. J. Han, and S. M. Wang, "Microscopic analysis of expansion mechanism of weathered red sandstone in Hongshanyao," *Rock and Soil Mechanics*, vol. 30, no. S2, pp. 192–195, 2009.

[14] Z. D. Zhu, F. D. Xing, Y. Zhang, and W. Z. Chen, "Experimental study on wetting characteristics of expansive red sandstone in Hongshanyao," *Rock and Soil Mechanics*, vol. 7, pp. 1014–1018, 2005.

[15] J. Yu, S. J. Chen, X. Chen, Y. Z. Zhang, and Y. Y. Cai, "Experimental investigation on mechanical properties and permeability evolution of red sandstone after heat treatments," *Journal of Zhejiang University-Science A (Applied Physics & Engineering)*, vol. 16, no. 9, pp. 749–759, 2015.

[16] L. Ma and Y. F. Hu, "Study on reinforcement methods based on different disintegration mechanism of red sandstone landslides in Changji Highway," *Advanced Materials Research*, vol. 838-841, pp. 840–845, 2013.

[17] Z. L. Zhao, H. W. Jing, G. P. Fu, Q. Yin, X. Shi, and Y. Gao, "Experimental and numerical studies on permeability properties of thermal damaged red sandstone under different confining pressures," *Geofluids*, vol. 2021, Article ID 6693768, 13 pages, 2021.

[18] L. J. Yin, F. D. Zhao, Z. Q. Liu, Y. P. Zhu, and S. L. Kan, "Study on factors influencing the disintegration rate and disintegration mechanism of red sandstone," *Geotechnics*, vol. S2, pp. 1–12, 2020.

[19] H. Y. Wang, J. Y. Xu, P. Wang, S. Liu, and S. H. Liu, "Study on mechanical properties and energy mechanism of red sandstone under hydrodynamic coupling," *Geotechnical Mechanics*, vol. 37, no. 10, pp. 2861–2868, 2016.

[20] H. Y. Wang, W. X. Ding, and J. J. Yang, "Study on the engineering properties of saturated red sandstone[J]," *Applied Mechanics & Materials*, vol. 638-640, pp. 589–593, 2014.

[21] J. Q. Jiang, "Field tests on mechanical characteristics and strength parameters of red-sandstone," *Journal of Central South University (English version)*, vol. 17, pp. 381–387, 2010.

[22] Z. C. Tang, Q. Z. Zhang, and Y. Zhang, "Cyclic Drying–Wetting Effect on Shear Behaviors of Red Sandstone Fracture," *Rock Mechanics and Rock Engineering*, vol. 9, 2021.

[23] M. H. Zhao, J. Y. Deng, and W. G. Cao, "Research on the disintegrating characteristics of red sandstone and its landfill technology," *China Highway Journal*, vol. 3, pp. 2–6, 2003.

[24] W. G. Zuo, *Study on the Engineering Properties of the Cretaceous and Tertiary Red Beds in Hunan*, Central South University, 2006.